

Partial pyrolysis of olive wood to improve its sorption of chlorophenols and nitrophenols

A. H. El-Sheikh

Received: 9 August 2012 / Revised: 12 March 2013 / Accepted: 6 May 2013 / Published online: 25 May 2013
© Islamic Azad University (IAU) 2013

Abstract Partial pyrolysis alters the chemical and textural properties of the lignocellulosic material. This work reports the effect of partial pyrolysis of olive wood on adsorption isotherms, kinetics and thermodynamics of chloro and nitrophenols. Shape of adsorption isotherms of the partially pyrolyzed sorbents was L3 for phenol; L2 for 2-nitrophenol and 2,4-dinitrophenol; H3 for 2-chlorophenol, 3-chlorophenol and 4-nitrophenol; and H2 for 4-chlorophenol. The pyrolyzed olive wood sorbents obeyed Langmuir and Freundlich models. Pyrolysis raised adsorption capacity, favorability and spontaneity; the adsorption became more exothermic; the randomness decreased. The adsorption was mainly physical; it occurred first by film diffusion then by pore-filling. Adsorption followed second-order rate kinetics. Adsorption of phenols on olive wood seemed to be governed by hydrophobic interaction. Washing the pyrolyzed olive wood with ethanol caused a decrease in adsorption capacity, favorability and spontaneity, and the adsorption became less exothermic. This indicated that pyrolysis produced species on the olive wood surface that played a significant role in phenols adsorption.

Keywords Adsorption models · Olive wood · Phenols · Pyrolysis

Introduction

Olive wood is considered an important agricultural waste product in the Mediterranean area. This is due to the

widespread cultivation of olives and to huge amounts of wood produced from pruning process every year. Olive wood has many uses: an energy source, a sugar source for bioethanol production, and for the production of cellulose kraft pulp and activated carbon. Environmentalists have used olive waste materials for uptake of metal ions from aqueous solutions (de Hoces et al. 2006; Saka et al. 2012). Modification of lignocellulosic sorbents by physical and/or chemical methods may affect its chemical and textural properties.

For example, Shin et al. (2005) reported modification of lignocellulosic sorbents with lanthanum for orthophosphate treatment. Martin-Lara et al. (2008) reported modification of olive waste with phosphoric acid and hydrogen peroxide for improving adsorption of copper and cadmium. Abia et al. (2003) reported modification of cassava waste biomass with thioglycolic acid to improve the adsorption of cadmium, copper and zinc. Raji and Amirudhan (1998) reported modification of sawdust with polyacrylamide for chromium (VI) adsorption. Igwe et al. (2005) reported carboxymethylation and thiolation of coconut fiber and sawdust for the adsorption of lead, mercury and arsenic ions in water. Zghida et al. (2006) reported the cationization of cotton fibers, wood sawdust and maize-cob flour for removing anionic surfactants from water.

Pyrolysis is a physical process which involves heating a carbonaceous material at high temperature under inert atmosphere. Pyrolysis was widely used for the preparation of activated carbon (El-Sheikh et al. 2004). If the lignocellulosic sorbent is heated at low temperature under inert atmosphere, this will partially change the chemical and textural characteristics of the sorbent without forming activated carbon. This is called partial pyrolysis.

Phenolic compounds are toxic compounds. Some are suspected human carcinogens (EPA 1988). They may

A. H. El-Sheikh (✉)
Department of Chemistry, Faculty of Science, Hashemite
University, Zarqa 13115, Jordan
e-mail: amjadelsheikh3@yahoo.com

present in the wastewater generated from paint, petrochemical, pharmaceutical, plastic, rubber proofing, pesticide, iron steel, phenol production, paper and pulp industries (Ahmaruzzaman 2008). Long-term exposure to them may cause loss of appetite, headache and rapid fatigue. United States Environmental Protection Agency called for lowering phenol content in wastewater to less than 1 mg L^{-1} .

Traditionally, adsorption by activated carbon was the most efficient method for the removal of phenolic compounds from water. Recently, microorganisms have been considered promising biosorbents of phenols (Brandt et al. 1997). Various sorption processes may be involved: adsorption, ion exchange and covalent bonding (Fourest and Volesky 1997). Unfortunately, the use of microorganisms may cause fatal diseases. Alternatively, the use of agricultural waste material is safer and renewable. It also solves waste disposal problem. Sorption of phenols was reviewed by Ahmaruzzaman (2008) and by Mathialagan and Viraraghavan (2008). Sorption of phenol and 2-chlorophenol on *Funalia trogii* pellets was investigated by Bayramoglu et al. (2009). Vazquez et al. (2007) reported adsorption of phenol on formaldehyde-pretreated *Pinus pinaster* bark. Wu and Yu (2006) studied adsorption of 2,4-dichlorophenol from aqueous solution on *Phanerochaete chrysosporium* biomass. This is in addition to many other works (Navarro et al. 2008; Aravindhan et al. 2009; Nadavala et al. 2009).

In adsorption studies, it is critical to investigate the shape of isotherms, equilibrium, kinetic and thermodynamic parameters of the adsorption process. This will help better understand the adsorption characteristics. Some researchers reported the kinetics of phenols adsorption on various biosorbents (Wu and Yu 2006; Vazquez et al. 2007; Bayramoglu et al. 2009; Nadavala et al. 2009). Other works reported thermodynamics of phenols adsorption (Wu and Yu 2006; Aravindhan et al. 2009; Bayramoglu et al. 2009).

In this work, the effect of pyrolysis of olive wood at various temperatures on its adsorption properties toward seven phenolic compounds is investigated. The following chlorophenols and nitrophenols were selected because they have a wide range of pK_a values: phenol: 9.89; 2-chlorophenol: 8.5; 3-chlorophenol: 8.8; 4-chlorophenol: 9.2; 2-nitrophenol: 7.17; 4-nitrophenol: 7.15; 2,4-dinitrophenol: 4.96. It is proposed that pyrolysis will change the surface chemistry and textural properties of the olive wood surface. While volatile components will be vaporized, chemical degradation of some constituents may also occur. So that further washing of the pyrolyzed sorbent may be necessary to uncover the pyrolyzed surface. This will elucidate the role of the compounds covering the pyrolyzed olive wood

surface in the adsorption process. Parameters of Langmuir and Freundlich adsorption models, free energy of adsorption, kinetic and intraparticle diffusion parameters, and thermodynamic parameters (ΔG° , ΔH° and ΔS°) will be studied in this work. All experiments were conducted at pH 7 in this work because it was the optimum pH for solid phase extraction of those phenols on olive wood in our previous work (El-Sheikh et al. 2011). This work was done during the period from February to October 2010 at the department of chemistry/The Hashemite University/Zarqa/Jordan.

Materials and methods

Chemicals and materials

Chemicals used in this work were purchased from the following resources: phenol (Ph) from POCH (Poland); 2-chlorophenol (2-CP) and 4-chlorophenol (4-CP) from Fluka (Italy); 3-chlorophenol (3-CP) and 2,4-dinitrophenol (2,4-DNP) from ACROS (Belgium); 2-nitrophenol (2-NP) from Aldrich (Germany); 4-nitrophenol (4-NP) from Merck (Germany); ethanol and n-hexane from TEDIA (USA); and diethyl ether from Scharlau (Spain). Olive wood used in this work was collected from olive trees grown in Tareq area at the capital city Amman. Olive wood was cut into small pieces, ground with a blender and then passed through a 1.0 mm sieve. That was considered as the unpyrolyzed olive wood.

Pyrolysis of olive wood

The raw (unpyrolyzed) olive wood was used to prepare pyrolyzed olive wood; 10.0 g raw (unpyrolyzed) olive wood was placed inside a furnace under inert atmosphere (N_2 gas flowing at 8.0 L min^{-1}). Pyrolysis was conducted at various temperatures: 100, 150, 200, 250 and 300 °C. Pyrolysis was done by flowing N_2 gas for 15 min, and then the furnace was turned on and adjusted to the desired temperature. The temperature was maintained for 1 h after which the furnace was switched-off and N_2 gas flow was maintained until furnace temperature reached room temperature.

For the sake of removing any compounds covering the pyrolyzed adsorbents' surface, the produced sorbents were washed. Washing pyrolyzed olive wood was conducted by agitating the pyrolyzed olive wood with 50 ml of the desired solvent for 2 h. The UV–VIS spectrum of the wash was recorded and the process was repeated several times until absorption spectrum was identical with that of the pure washing solvent. The washed-pyrolyzed sorbents were then dried at 150 °C to remove any traces of ethanol. The

produced adsorbents were labeled according to the pyrolysis temperature followed by washing solvent. So that three sets of olive wood were used in this work:

- Unpyrolyzed olive wood (OW).
- Pyrolyzed only olive wood at various temperatures: raw unpyrolyzed olive wood, OW-100, OW-150, OW-200, OW-250 and OW-300.
- Pyrolyzed olive wood at various temperatures followed by ethanol washing: OW-100-ethanol, OW-150-ethanol, OW-200-ethanol, OW-250-ethanol and OW-300-ethanol.

Equilibrium adsorption experiments

Batch adsorption experiments were conducted for each phenolic compound separately to estimate the equilibrium adsorption parameters and thermodynamic constants for the adsorption of each phenolic compound on the unpyrolyzed and pyrolyzed olive wood sorbents. To reach this purpose, masses of 50 mg of the adsorbent were mixed with 25 mL solutions of certain phenolic compound (concentration range 0–25 mg L⁻¹) in 50-ml-conical flasks at pH 7.0. Tightly closed flasks were shaken for 24 h at 30, 50 or 70 °C to reach equilibrium using a thermo-stated shaker (GFL 1083, Germany). The remaining concentrations of the phenolic compound at equilibrium (C_e) were estimated spectrometrically using a Cary 100Bio UV–VIS spectrophotometer at the following wavelength values: Ph: 270 nm; 2-CP and 3-CP: 276 nm; 4-CP: 282 nm; 2-NP: 278 nm; 4-NP: 316 nm; 2,4-DNP: 354 nm. The amount of the phenolic compound removed per unit mass of sorbent at equilibrium (q_e , mg g⁻¹) was calculated using the following equation:

$$q_e = [C_o - C_e]V/m$$

where C_o is the initial phenolic compound concentration (mg L⁻¹), V is the total volume of mixture (L), and m is the mass of sorbent (g).

Batch kinetic experiments

Kinetic adsorption experiments were conducted as follows: 500 mg of the adsorbent was stirred at 30 °C with 500 mL solution of 15 mg L⁻¹ of the desired phenolic compound at pH 7. The decay in phenolic compound concentration was followed by withdrawing 3 mL samples from the mixture using a pipette at certain time intervals (t), and then the phenolic compound concentration at that time (C_t) was determined spectrometrically as described in “[Equilibrium adsorption experiments](#).” The adsorbed amount of the phenolic compound on the adsorbent (q_t) at time t was estimated (mg g⁻¹) using the equation:

$$q_t = [C_o - C_t]V/m$$

Evaluation of adsorption data

Equilibrium adsorption isotherm models

Langmuir model Langmuir assumes that the surface is homogenous. The linear Langmuir equation may be written as follows (Langmuir 1918):

$$\frac{C_e}{q_e} = \frac{1}{bQ_{\max}} + \frac{C_e}{Q_{\max}}$$

where C_e is the remaining concentration of phenolic compound at equilibrium in the solution (mg L⁻¹), q_e is the amount of phenolic compound adsorbed per unit mass of sorbent at equilibrium (mg g⁻¹), Q_{\max} is the amount of adsorbate at complete monolayer coverage (mg g⁻¹), and b is the equilibrium adsorption constant (L mg⁻¹), which represents the ratio of adsorption and desorption rate constants. Higher values of b indicate more favorable adsorption. Evaluation of Q_{\max} and b was conducted by plotting (C_e/q_e) against C_e and then linear regression.

Freundlich model Freundlich assumes heterogeneous surface. Freundlich isotherm model can be represented by the following linear equation (Freundlich 1906; Sanchez et al. 1999):

$$\log q_e = \log K_F + n \log C_e$$

where K_F (mg¹⁻ⁿ g⁻¹ Lⁿ) represents the sorption capacity when equilibrium concentration equals to 1, and n represents the degree of dependence of sorption on equilibrium concentration. n is an indicator of sorption intensity, surface heterogeneity and adsorption favorability (Frimmel and Huber 1996). Lower values of n reflect higher heterogeneity of the adsorbent surface and that sorption is favorable over the entire studied concentrations range (Frimmel and Huber 1996). Evaluation of K_F and n values was conducted by plotting $\log q_e$ against $\log C_e$ and then linear regression.

Kinetic parameters

The adsorption kinetics of the phenolic compounds was evaluated by applying two kinetic models to fit the concentration decay of phenolic compounds with time: the pseudo-first-order model (Lagergren 1898) and pseudo-second-order model (Ho and Mckay 2000). The experimental value of q_e was estimated by extrapolating the experimental data to $t = \infty$.

Pseudo-first-order kinetics According to Lagergren (1898), pseudo-first-order kinetic equation may take the following linear form:



$$\log(q_e - q_t) = \log q_e - (k_1/2.303)t$$

where q_e and q_t (both in mg g^{-1}) are the amounts of phenolic compounds adsorbed at equilibrium and at time t (minutes), and k_1 is the pseudo-first-order rate constant (min^{-1}). k_1 may be found by plotting $\log(q_e - q_t)$ versus t and then linear regression.

Pseudo-second-order kinetics The pseudo-second-order kinetics may be expressed using the following equation (Ho and McKay 2000):

$$t/q_t = (1/k_2 q_e^2) + (1/q_e)t$$

where k_2 ($\text{g mg}^{-1} \text{min}^{-1}$) is the second-order rate constant of adsorption. The values of k_2 and q_e can be estimated experimentally from the slope and intercept of the plot t/q_t versus t .

Adsorption mechanism

It is important in adsorption studies to understand whether adsorption occurs through chemisorption process or physisorption process. This may be predicted by following the free energy of adsorption (E). Furthermore, it is important to decide which step is the rate determining step: film diffusion or pore diffusion.

Free energy of adsorption (E) Free energy of adsorption (E) ($\text{mol}^2 \text{J}^{-2}$) was estimated by applying Dubinin–Radushkevich model (Nadavala et al. 2009), which is represented by the following linear equation:

$$\ln q_e = \ln q_m - B\varepsilon^2$$

where $\varepsilon = RT \ln(1 + (1/C_e))$; B is a constant that is related to E (J mol^{-1}) where $E = (-2B)^{-1/2}$ (Bansode et al. 2004); R is the gas constant ($8.314 \text{ J mol}^{-1} \text{K}^{-1}$); and T is the temperature (K). The values of B were found by plotting $\ln q_e$ against ε^2 and then linear regression. The adsorption mechanism may be predicted by following the value of E : If E is between 8 and 16 kJ mol^{-1} , then the adsorption occurs mainly through chemisorption (ion exchange) process. If $E < 8 \text{ kJ mol}^{-1}$, then the adsorption process has mainly physical nature (Sanchez et al. 1999).

Intraparticle diffusion Kinetic data can be used to specify the mechanism of adsorption (Wu and Yu 2006; Aravindhan et al. 2009). For solid–liquid adsorption, either film diffusion or intraparticle diffusion or both usually control the solute transfer process. The sorption rate will be generally controlled by the slowest step (Aravindhan et al. 2009). The intraparticle (pore) diffusion may be the rate-limiting step of the adsorption process. This may be

confirmed by applying Morris–Weber equation (Weber and Morris 1963):

$$q_t = k_{id} \cdot t^{0.5}$$

where k_{id} is the intraparticle transport constant ($\text{mg g min}^{-1/2}$) of the phenolic compound. If a straight line passing through the origin is obtained, then the intraparticle diffusion is the only rate-limiting step. If biphasic plot is obtained, film diffusion (first linear portion of the plot usually of steeper slope) occurs first and then pore diffusion (second linear portion of the plot usually of lower slope) follows. The slope of the second portion represents k_{id} .

Thermodynamic parameters

Thermodynamic properties of the adsorption system were estimated by conducting the sorption experiments at different temperatures (30, 50 and 70 °C). The effect of temperature on adsorption of various phenolic compounds on olive wood-based adsorbents was studied by applying the following equations:

$$\ln K_c = (-\Delta H^\circ/RT) + (\Delta S^\circ/R) \quad \text{and} \\ \Delta G^\circ = -RT \ln K_c$$

where ΔH° (kJ mol^{-1}), ΔS° ($\text{kJ mol}^{-1} \text{K}^{-1}$), ΔG° (kJ mol^{-1}), T (K) and K_c are enthalpy, entropy, Gibbs free energy, absolute temperature and equilibrium constant, respectively, R is the gas constant ($8.314 \text{ J mol}^{-1} \text{K}^{-1}$), and K_c is the thermodynamic equilibrium constant which reflects the ability and capacity of the adsorbent to retain the phenolic compound. This constant is determined by plotting $\ln(q_e/C_e)$ against q_e and extrapolating to $q_e = 0$ (Khan and Singh 1987). ΔG° reflects the adsorption spontaneity. It also indicates that physical adsorption is taking place if ΔG° ranges from -20 to 0 kJ mol^{-1} or chemisorption is taking place if ΔG° ranges from -80 to -400 kJ mol^{-1} . By plotting $\ln K_c$ against $(1/T)$, straight lines were obtained from which ΔH° and ΔS° were calculated from the slope and intercept of the plots, respectively. The value of ΔH° reflects the enthalpy of the reaction (exothermic or endothermic reaction). The value of ΔS° reflects the change in randomness and disorder of the adsorption process.

Results and discussion

Characteristics of unpyrolyzed and pyrolyzed olive wood

The purpose of the present work is to study the effect of partial pyrolysis of olive wood on its kinetic, thermodynamic and equilibrium adsorption properties toward chlorophenols and nitrophenols. This is based on the hypothesis that pyrolysis alters the chemical composition of the olive

wood by forcing chemical degradation of the olive wood. This may produce new compounds that play role or retard the adsorption process. It was shown in a previous work (El-Sheikh et al. 2011) that olive wood contains 6.9 % moisture; 1.8 % hemicelluloses; 42.0 % α -cellulose; 44.0 % lignin; 1.4 % ash content; 49.9 % C; and 44.0 % O. After pyrolysis: the carbon content has increased and the oxygen content has decreased due to significant loss of volatile compounds and water. Almost 63 % of the OW mass was lost after pyrolysis at 300 °C (El-Sheikh et al. 2011).

Pyrolysis will surely affect the chemical and structural properties of the olive wood. It was reported by Hajaligol et al. (2002) that the temperature range (250–400 °C) is responsible for primary decomposition (thermolysis) of the lignocellulosic material. Bridgwater (1994) reported that cellulose degradation starts at 200 °C by β -elimination of the cellulose hydroxyl groups. The IR spectra showed a significant decrease in O–H stretching band peak height at 200 °C. This indicated loss of water originally adsorbed or formed by β -elimination. As temperature increases, the symmetrical and asymmetrical stretching of etheric group at $\sim 1,240$, 1,160 and 1,050 cm^{-1} disappeared, which indicate further destruction of cellulose. At higher temperatures, random bond cleavage of cellulose caused formation of low molecular weight compounds. Bridgwater (1994) reported that the production of volatile compounds ends at 450 °C and aromatization reactions start forming carbon. However, in this work, it was aimed not to allow the formation of carbon. According to Bridgwater (1994), degradation of hemicellulose starts by decomposition of the polymeric chain into water-soluble fragments, then to monomeric units and then into volatile compounds. This occurs between 220 and 320 °C. Unfortunately, in our study, we could not support this hypothesis by IR data. The degradation of lignin starts by breaking aliphatic bonds to release tar hydrocarbon compounds (Bridgwater 1994). Secondary reactions (cracking and polymerization) then take place. This was indicated by the appearance of the C=C stretching of symmetrical conjugated diene band at 1,620–1,625 cm^{-1} at 250 °C. Not only will the chemical properties be affected, but also the textural properties. Grioui et al. (2007) reported that pyrolysis increases the porosity of the pyrolyzed lignocellulosic sorbents especially in the range 250–275 °C. However, in our previous work (El-Sheikh et al. 2011), we have reported that the methylene blue relative surface area has decreased after pyrolysis. It was reported that olive wood may contain variety of compounds, such as hydroxytyrosol, tyrosol, cycloolivil, 7-deoxyloganic acid, oleuropein and ligstroside (Perez-Bonilla et al. 2006). The presence of some metals (alkali, earth alkaline and transition metals) in the olive wood may due to the decomposition of these compounds totally or partially. So that gaseous products such as CO_2 , CO , H_2 , C_2H_2 , C_2H_4 and C_2H_6 (Overend and Chornet 1999) may be

elevated, and thus, porosity of the olive wood may be affected. It was also shown (El-Sheikh et al. 2011) that pyrolysis increased the surface acidity but decreased the surface basicity. This may reflect negligible responsibility of the textural properties and surface area toward phenols adsorption. On the contrary, the surface functional groups probably play the major role in phenols adsorption.

Equilibrium adsorption isotherms of phenols on olive wood

Unpyrolyzed olive wood

From the adsorption data presented in Table 1, adsorption of various phenols on unpyrolyzed olive wood was best represented by Freundlich isotherm model as indicated by $R^2 > 0.9755$, while Langmuir isotherm model gave R^2 between 0.4921 and 0.8903. The adsorption was favored over the entire concentration range and the surface was heterogeneous and the energy of the active sites was variable as indicated by n values less than 1 (Frimmel and Huber 1996). The values of mean free energy of adsorption of unpyrolyzed olive wood (E) are shown in Table 1. They were in the range 2,236–2,887 J mol^{-1} . This indicated the physical nature for the adsorption of all the phenols on unpyrolyzed olive wood (Sanchez et al. 1999).

Pyrolyzed olive wood

From Table 1, it was generally noted that Freundlich model best represented adsorption of Ph, 2-NP and 2,4-DNP on pyrolyzed olive wood, while Langmuir model best represented adsorption of 2-CP, 3-CP, 4-CP and 4-NP on pyrolyzed olive wood. From K_F values, it was noted that thermal treatment has almost doubled adsorption capacity of the olive wood. Pan and Xing (2008) reported that when H-bonds are predominant, a decrease in the oxygen-containing groups on the adsorbent surface would decrease the adsorption. This will offer less polar–polar and ion-exchange type interaction with phenols. This will inhibit adsorption of more polar phenolic compounds. On the other hand, for adsorption controlled by hydrophobic interactions, the decrease in oxygen content would increase the accessibility and affinity of phenols toward the less polar surface. So that adsorption of phenols on olive wood seemed to be governed by hydrophobic interaction.

Surface heterogeneity, variability in active sites and favorability of adsorption at the entire concentration range are still predominant as indicated by n values less than 1. The adsorption became more favored since b values have increased after pyrolysis. It was generally noted that the adsorption capacity (K_F values) and favorability (b values) of chlorophenols are higher than those of nitrophenols.



Table 1 Parameters of adsorption isotherms of various phenols on unpyrolyzed and pyrolyzed olive wood sorbents

	Type	E (J mol ⁻¹)	Langmuir model			Freundlich model		
			b (L mg ⁻¹)	Q_{\max} (mg g ⁻¹)	R^2	K_F (mg ¹⁻ⁿ g ⁻¹ mg L ⁿ)	n	R^2
Ph								
Unpyrolyzed	L3	2,236	0.18	7.6	0.6567	1.2	0.63	0.9878
OW-100	L3	2,500	0.27	8.5	0.8128	1.7	0.56	0.9783
OW-150	L3	3,162	0.30	8.1	0.8007	1.8	0.52	0.9808
OW-200	L3	2,500	0.24	8.4	0.7857	1.6	0.58	0.9782
OW-250	L3	2,887	0.28	8.1	0.8039	1.7	0.54	0.9850
OW-300	L3	2,673	0.27	8.2	0.7848	1.7	0.55	0.9755
2-CP								
Unpyrolyzed	L1	2,236	0.14	12.8	0.7734	1.5	0.72	0.9971
OW-100	H3	2,887	1.04	8.8	0.9634	3.4	0.51	0.8794
OW-150	H3	2,673	0.84	9.0	0.9513	3.2	0.52	0.8350
OW-200	H3	2,500	0.75	8.9	0.9520	3.0	0.53	0.8396
OW-250	H3	2,887	0.94	8.6	0.9604	3.2	0.51	0.8594
OW-300	H3	2,673	0.78	8.9	0.9506	3.1	0.53	0.8298
3-CP								
Unpyrolyzed	L1	2,887	0.27	10.6	0.8903	2.0	0.62	0.9978
OW-100	H3	3,536	1.43	8.6	0.9666	3.7	0.47	0.9149
OW-150	H3	2,887	1.06	8.8	0.9624	3.5	0.50	0.8519
OW-200	H3	2,887	0.97	8.6	0.9611	3.3	0.50	0.8454
OW-250	H3	3,536	1.24	8.5	0.9660	3.5	0.48	0.8771
OW-300	H3	2,887	1.00	8.7	0.9618	3.4	0.50	0.8395
4-CP								
Unpyrolyzed	L1	2,887	0.26	12.1	0.8717	2.2	0.65	0.9933
OW-100	H2	3,162	1.15	11.1	0.9877	4.8	0.59	0.9107
OW-150	H2	2,887	0.97	11.3	0.9726	4.6	0.61	0.8783
OW-200	H2	2,887	0.80	11.6	0.9239	4.3	0.61	0.8525
OW-250	H2	3,162	1.11	11.1	0.9736	4.7	0.58	0.8868
OW-300	H2	2,887	0.88	11.6	0.9390	4.5	0.61	0.8516
2-NP								
Unpyrolyzed	L4	2,236	0.10	6.1	0.6765	0.7	0.59	0.9755
OW-100	L2	5,000	0.27	5.9	0.9065	1.2	0.52	0.9797
OW-150	L2	2,500	0.28	5.8	0.9074	1.2	0.52	0.9773
OW-200	L2	2,357	0.27	5.8	0.9026	1.2	0.53	0.9799
OW-250	L2	2,673	0.29	5.7	0.9088	1.3	0.50	0.9812
OW-300	L2	2,500	0.29	5.7	0.9014	1.2	0.51	0.9788
4-NP								
Unpyrolyzed	L1	2,236	0.078	17.2	0.4921	1.2	0.81	0.9825
OW-100	H3	2,357	0.61	9.4	0.9573	2.9	0.57	0.8849
OW-150	H3	2,357	0.55	9.5	0.9439	2.8	0.58	0.8686
OW-200	H3	2,236	0.49	9.5	0.9359	2.6	0.59	0.8641
OW-250	H3	2,500	0.54	9.4	0.9538	2.7	0.59	0.8888
OW-300	H3	2,357	0.50	9.7	0.9554	2.6	0.60	0.8901
2,4-DNP								
Unpyrolyzed	L4	2,236	0.094	6.1	0.6430	0.7	0.62	0.9803
OW-100	L2	5,000	0.26	5.8	0.9011	1.2	0.53	0.9741
OW-150	L2	2,357	0.27	5.8	0.9015	1.2	0.53	0.9680
OW-200	L2	2,887	0.26	5.7	0.8859	1.2	0.50	0.9814
OW-250	L2	2,673	0.29	5.6	0.8944	1.2	0.49	0.9692
OW-300	L2	2,673	0.28	5.6	0.8784	1.2	0.49	0.9661

Table 2 Parameters of adsorption isotherms of pyrolyzed-ethanol-washed olive wood sorbents

	Type	E (J mol ⁻¹)	Langmuir model			Freundlich model		
			b (L mg ⁻¹)	Q_{\max} (mg g ⁻¹)	R^2	K_F (mg ¹⁻ⁿ g ⁻¹ mg L ⁿ)	n	R^2
Ph								
OW-100-ethanol	L1	3,162	0.24	7.5	0.8187	1.3	0.51	0.9896
OW-150-ethanol	L1	2,673	0.22	7.6	0.810	1.3	0.58	0.9849
OW-200-ethanol	L1	4,082	0.18	8.0	0.7636	1.4	0.52	0.9190
OW-250-ethanol	L1	4,082	0.20	7.9	0.7916	1.4	0.52	0.9253
OW-300-ethanol	L1	2,887	0.23	7.5	0.8265	1.5	0.50	0.9368
2-CP								
OW-100-ethanol	L1	2,887	0.20	10.8	0.7835	1.7	0.57	0.9448
OW-150-ethanol	L1	2,500	0.18	11.3	0.7973	1.7	0.65	0.9814
OW-200-ethanol	L1	3,162	0.11	14.0	0.6832	1.4	0.74	0.9780
OW-250-ethanol	L1	3,536	0.13	12.9	0.7503	1.5	0.71	0.9809
OW-300-ethanol	L1	2,357	0.15	12.1	0.7765	1.6	0.68	0.9817
3-CP								
OW-100-ethanol	L1	2,887	0.24	10.4	0.8227	1.8	0.57	0.9611
OW-150-ethanol	L1	2,673	0.22	10.6	0.8128	1.7	0.65	0.9854
OW-200-ethanol	L1	4,082	0.15	12.0	0.7434	1.6	0.67	0.9778
OW-250-ethanol	L1	5,000	0.18	11.4	0.7929	1.6	0.66	0.9834
OW-300-ethanol	L1	2,673	0.19	11.1	0.7977	1.7	0.64	0.9799
4-CP								
OW-100-ethanol	L1	4,082	0.26	11.4	0.7199	2.2	0.56	0.9497
OW-150-ethanol	L1	3,162	0.23	11.9	0.7038	2.1	0.61	0.9631
OW-200-ethanol	L1	5,000	0.16	13.5	0.6221	1.8	0.65	0.9658
OW-250-ethanol	L1	7,071	0.21	12.1	0.6617	2.1	0.58	0.9543
OW-300-ethanol	L1	3,536	0.21	12.1	0.6756	2.1	0.60	0.9588
2-NP								
OW-100-ethanol	L4	2,236	0.22	4.4	0.8737	0.82	0.52	0.9625
OW-150-ethanol	L4	2,236	0.24	4.3	0.8803	0.85	0.53	0.9647
OW-200-ethanol	L4	4,082	0.18	4.5	0.8621	0.80	0.53	0.9648
OW-250-ethanol	L4	4,082	0.20	4.5	0.8735	0.86	0.52	0.9640
OW-300-ethanol	L4	2,236	0.22	4.4	0.8754	0.89	0.50	0.9654
4-NP								
OW-100-ethanol	L1	2,357	0.15	11.6	0.7757	1.4	0.71	0.9774
OW-150-ethanol	L1	2,236	0.13	12.6	0.7211	1.3	0.76	0.9777
OW-200-ethanol	L1	3,162	0.10	14.2	0.5842	1.3	0.70	0.9646
OW-250-ethanol	L1	3,162	0.11	14.0	0.6712	1.3	0.75	0.9680
OW-300-ethanol	L1	2,236	0.12	13.1	0.7672	1.4	0.74	0.9752
2,4-DNP								
OW-100-ethanol	L4	2,236	0.20	4.5	0.8899	0.75	0.58	0.9788
OW-150-ethanol	L4	2,236	0.21	4.4	0.8766	0.77	0.56	0.9716
OW-200-ethanol	L4	4,082	0.17	4.5	0.8788	0.76	0.55	0.9625
OW-250-ethanol	L4	4,082	0.20	4.4	0.8862	0.83	0.52	0.9607
OW-300-ethanol	L4	2,236	0.20	4.4	0.8734	0.84	0.52	0.9635

This was due to the fact that olive wood surface is negatively charged at pH 7 since its point of zero charge was in the range 5–7 (El-Sheikh et al. 2011). Since nitrophenols are more acidic (less pK_a values), then they will produce

more phenolate anions at pH 7, and more repulsion with the olive wood surface occurred. In case of nitrophenols, 2-NP and 2,4-DNP gave lower K_F and Q_{\max} values than 4-NP. This is probably due to the intramolecular hydrogen

bonding between the phenolic hydrogen and the oxygen of the nitro substituent in the ortho position. This makes the phenolic proton of 2-NP less available for interaction with the surface functional groups (El-Sheikh et al. 2011).

The adsorption capacities of the pyrolyzed olive wood sorbents toward phenols were comparable to some values reported by Aravindhan et al. (2009), such as sawdust-based activated carbon: 2.82 mg g^{-1} , and olive pomace: 5 mg g^{-1} . Free energy of adsorption (E) has generally increased after pyrolysis at almost all pyrolysis temperatures for all the phenols (see Table 1). However, all E values indicated physical adsorption was taking place. However, values reported for E in our work were lower than E values (12.5 kJ mol^{-1}) reported by Nadavala et al. (2009) for the adsorption of phenol on chitosan.

Ethanol washing of the pyrolyzed olive wood on the adsorption process

Pyrolysis of olive wood is expected to change the chemistry of the olive wood surface and may produce new species on the olive wood surface. These species may be adsorbed on the olive wood surface and may play a significant role in the adsorption process; they may enhance or inhibit the adsorption process. So that it was proposed that removing these species will affect the adsorption process positively or negatively depending on the role of these species in the adsorption process. Washing olive wood was conducted primarily to investigate the role of those species. Ethanol was selected for the washing process; it has a polarity index of $P^1 = 4.3$. Adsorption parameters are given in Table 2, from which it was noted that Freundlich model ($R^2 > 0.9190$) represented the data better than Langmuir model ($0.5842 < R^2 < 0.8899$). Compared to pyrolyzed only sorbents (OW-100, OW-150, OW-200, OW-250, OW-300), it was noted that K_F values have decreased after washing the pyrolyzed olive wood with ethanol. This indicated that the washed-up species that were produced by the pyrolysis process and adsorbed on olive wood surface played a significant role in the adsorption process of phenols. Removal of these species by washing has negatively affected the adsorption process. This was also supported by noting that b values have decreased after washing, which reflected a decrease in the adsorption favorability. n values still < 1 , which reflected heterogeneous surface. Free energy of adsorption (E) did not show clear trend after ethanol washing. However, values of E indicated that the adsorption still has physical nature.

Shape of adsorption isotherms

The adsorption isotherms of the phenolic compounds on unpyrolyzed, pyrolyzed, and pyrolyzed-then-washed olive

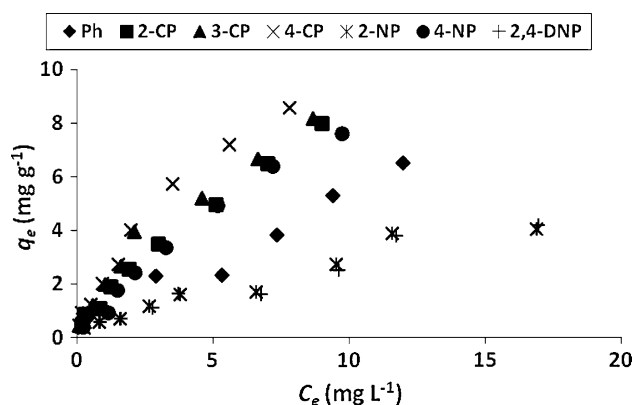


Fig. 1 Adsorption isotherms of various phenolic compounds on unpyrolyzed olive wood

wood adsorbents are shown in Figs. 1, 2 and 3. Classification of the isotherm types is presented in Tables 1 and 2. The adsorption isotherms of phenolic compounds on unpyrolyzed olive wood were all of L-type according to Giles and Smith (1974) classification. After pyrolysis, adsorption isotherms of 2-CP, 3-CP, 4-CP and 4-NP became of H-type, while Ph, 2-NP and 2,4-DNP maintained L-type isotherms. Washing after pyrolysis gave L-type isotherm for almost all the phenols according to Giles and Smith (1974) classification. L shape is considered the normal isotherm shape, which indicates that molecules adsorbed flat on the surface. H curve is a special case of the L curve, in which the solute has such high affinity so that in dilute solutions, it is completely adsorbed. The subgroups of these classes are arranged according to the shape of the curve part farther from the origin and the significance of plateau and changes of slope (Giles and Smith 1974). L2 and H2 curves indicate that as more sites in the substrate are filled, it becomes more difficult for solute molecules to find an empty available site. In L2 and H2 curves, the adsorbed solute molecules in the monolayer are so oriented that the new surface they present to the solution has low attraction for solute molecules (Giles and Smith 1974). This is reflected by the plateau in L2 and H2 curves, which represents first-degree saturation or complete monolayer coverage. If they are so oriented that the new surface has high attraction for more solute, then the curve rises steadily and has no plateau (L1). That was the case for 2-CP, 3-CP, 4-CP, 4-NP on unpyrolyzed olive wood and for almost all phenols on pyrolyzed-then-ethanol-washed olive wood sorbents. If new surface is developed, adsorption will continue until a second plateau is developed (L or H4-shapes), which represents the new saturation of the new surface. L4-shape was recorded for 2-NP and 2,4-DNP on unpyrolyzed olive wood and for 2-NP on pyrolyzed-then-ethanol-washed olive wood. If second saturation is not reached, then the curve appears as L3 or H3 shapes (Giles

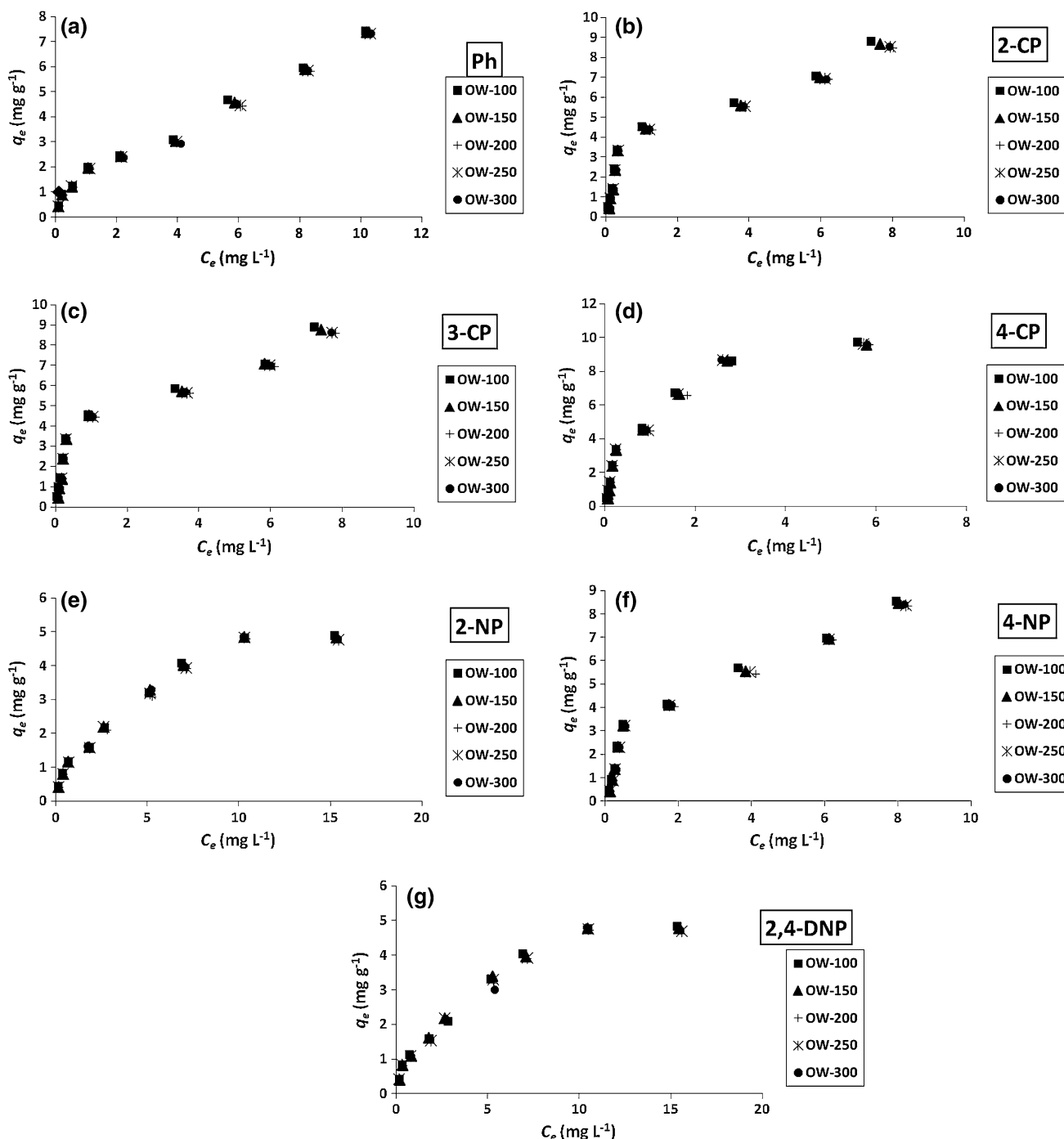


Fig. 2 Adsorption isotherms of various phenolic compounds on pyrolyzed olive wood adsorbents. **a** Ph; **b** 2-CP; **c** 3-CP; **d** 4-CP; **e** 2-NP; **f** 4-NP; **g** 2,4-DNP

and Smith 1974). L3-shape was the case for Ph on unpyrolyzed and pyrolyzed olive wood; H3-shape was the case for 2-CP, 3-CP and 4-NP on pyrolyzed olive wood.

Kinetic considerations

Adsorption of all the phenolic compounds on unpyrolyzed and pyrolyzed olive wood followed second-order rate

equation (see Table 3) in terms of high R^2 and agreement between $q_{e(\text{exp})}$ and $q_{e(\text{calculated})}$. The first-order rate law was not satisfactorily obeyed. Cruz et al. (2004) reported that the first-order adsorption kinetics is usually found within the first 30–50 min of the adsorption process. According to Morris–Weber equation, by plotting q_e versus $t^{0.5}$, biphasic plots, which do not pass through the origin, were observed (see Fig. 4). Three steps are taking place in the sorption process:

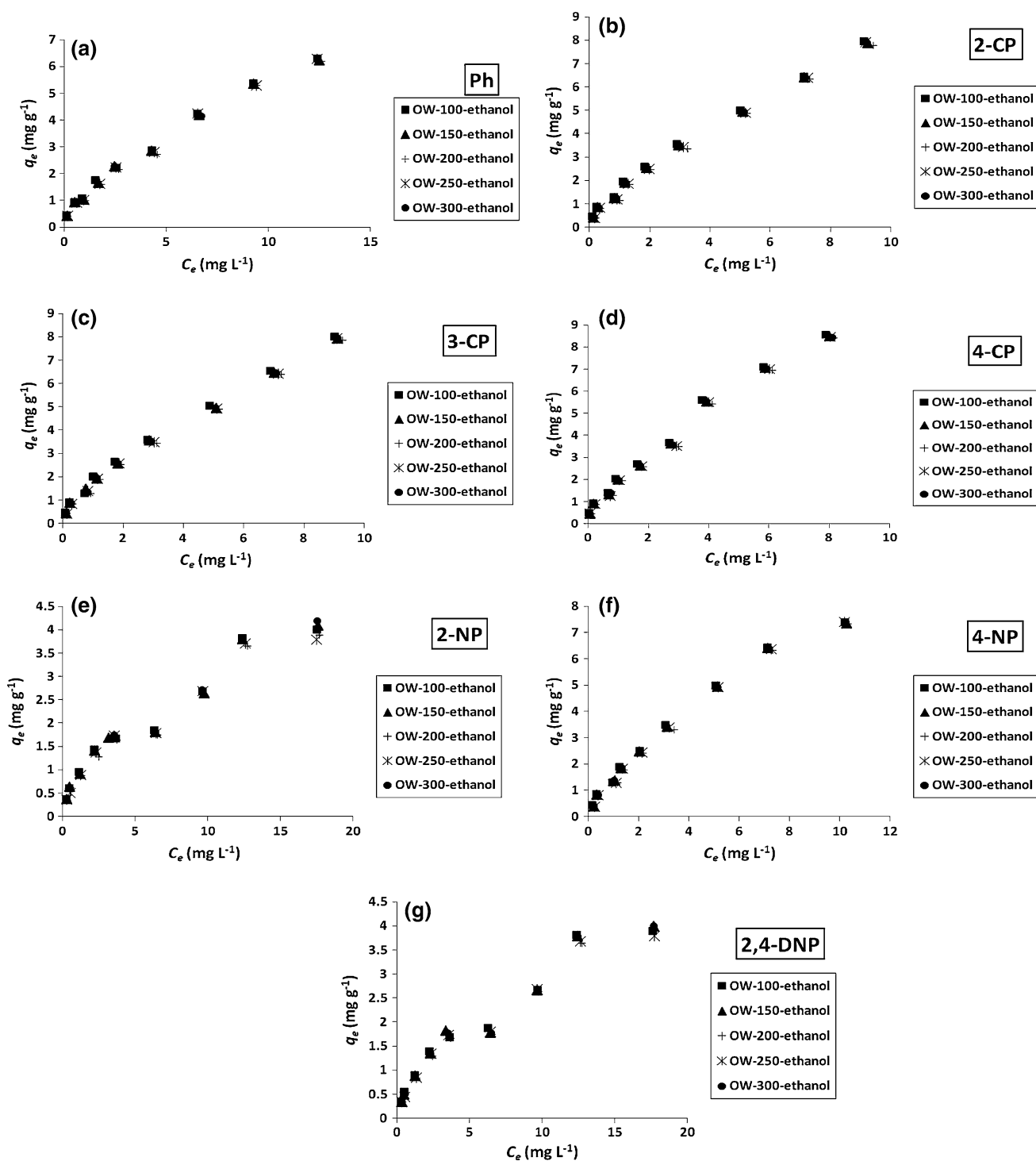


Fig. 3 Adsorption isotherms of various phenolic compounds on pyrolyzed-then-ethanol-washed olive wood adsorbents. **a** Ph; **b** 2-CP; **c** 3-CP; **d** 4-CP; **e** 2-NP; **f** 4-NP; **g** 2,4-DNP

first by film diffusion, then by intraparticle diffusion (pore diffusion), and then equilibrium was reached. Since a linear relationship between q_e and $t^{1/2}$ was observed over a period of time but did not pass through the origin, this suggested that intraparticle diffusion was present but not the only controlling step. From Table 3, it was noted that, compared to

unpyrolyzed olive wood, k_2 increased for Ph, 2-NP and 4-CP but decreased for 2-CP, 3-CP, 4-NP and 2,4-DNP. The intraparticle diffusion parameter (k_{id}) has decreased for all phenolic compounds except for Ph (see Table 1). This indicated that pyrolysis of olive wood slowed down the pore diffusion, and thus, it had more effect as a rate-limiting step.

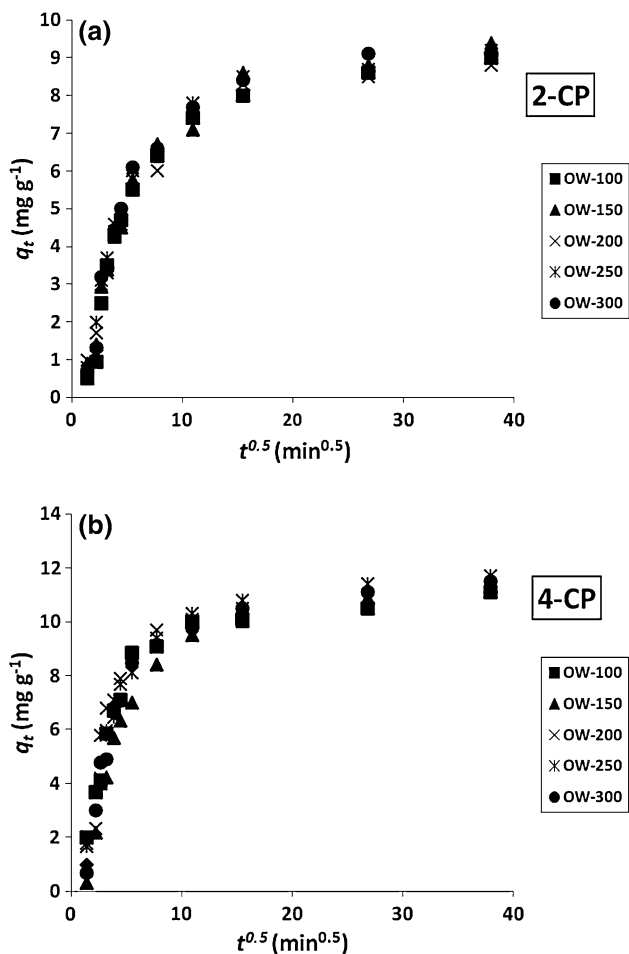
Table 3 Parameters of adsorption kinetics and thermodynamics of various phenols on unpyrolyzed and pyrolyzed olive wood sorbents

	ΔS° (J K ⁻¹ mol ⁻¹)	ΔH° (kJ mol ⁻¹)	ΔG° (kJ mol ⁻¹)			k_{id} (g mg ⁻¹ min ^{-0.5})	Second order	
			30 °C	50 °C	70 °C		k_2 ($\times 10^{-3}$) (g mg ⁻¹ min ⁻¹)	R^2
Ph								
Unpyrolyzed	-133.7	-46.7	-5.7	-2.6	-0.2	0.16	2.1	0.9990
OW-100	-72.1	-27.0	-5.4	-3.1	-2.6	0.28	6.9	0.9999
OW-150	-90.2	-32.9	-6.0	-2.9	-2.5	0.26	3.8	0.9977
OW-200	-53.8	-21.2	-5.4	-2.6	-3.4	0.30	3.8	0.9999
OW-250	-86.0	-31.1	-5.3	-2.8	-2	0.36	7.1	1.0000
OW-300	-89.2	-32.2	-5.4	-2.7	-1.9	0.32	3.3	0.9993
2-CP								
Unpyrolyzed	37.0	9.5	-1.7	-5.7	-3.5	0.42	8.8	0.9995
OW-100	-11.6	-11.9	-6.8	-11.9	-5.8	0.20	1.5	0.9415
OW-150	-12.9	-12.0	-6.6	-11.3	-5.6	0.18	2.8	0.9983
OW-200	-14.8	-12.0	-6.2	-10.4	-5.2	0.30	6.0	0.9995
OW-250	-21.6	-14.8	-6.6	-11.5	-5.3	0.28	3.3	0.9963
OW-300	-33.2	-18.7	-7.3	-10.9	-5.6	0.24	1.8	0.9832
3-CP								
Unpyrolyzed	-111.9	-38.0	-5.3	-2.1	-0.8	0.42	8.6	0.9991
OW-100	-181.0	-65.3	-10.7	-6.3	-3.6	0.24	3.9	0.9998
OW-150	-168.1	-61.1	-10.3	-6.7	-3.6	0.14	3.6	0.9985
OW-200	-165.8	-60.0	-9.8	-6.2	-3.2	0.12	2.8	0.9979
OW-250	-189.2	-68.0	-10.8	-6.5	-3.3	0.14	3.1	0.9977
OW-300	-172.5	-62.5	-10.4	-6.2	-3.6	0.14	2.5	0.8975
4-CP								
Unpyrolyzed	-116.1	-41.5	-5.5	-2.4	-0.6	0.44	3.3	0.9993
OW-100	-198.6	-70.6	-10.8	-5.5	-3.0	0.32	8.3	0.9998
OW-150	-238.1	-83.5	-12.1	-5.1	-2.7	0.22	3.1	0.9985
OW-200	-188.0	-66.4	-9.9	-4.6	-2.5	0.32	3.5	0.9997
OW-250	-219.6	-77.2	-11.3	-5.0	-2.6	0.30	8.9	0.9996
OW-300	-242.9	-85.0	-12.1	-5.0	-2.5	0.26	3.8	0.9993
2-NP								
Unpyrolyzed	-98.0	-33.5	-3.0	-1.2	0.9	0.40	4.3	0.9989
OW-100	-78.3	-28.3	-4.5	-3.1	-1.4	0.16	6.6	0.9997
OW-150	-81.9	-29.6	-4.7	-3.4	-1.4	0.14	3.1	0.9849
OW-200	-115	-39.8	-5.0	-2.7	-0.4	0.22	5.8	0.9995
OW-250	-71.9	-26.2	-4.5	-2.9	-1.6	0.22	5.5	0.9997
OW-300	-74.9	-27.5	-4.9	-3.0	-1.9	0.28	5.3	0.9996
4-NP								
Unpyrolyzed	-87.2	-28.7	-3.5	-1.6	-0.6	0.38	6.6	0.9989
OW-100	-177.8	-64.2	-10.7	-5.9	-3.7	0.16	1.9	0.9904
OW-150	-172.5	-62.4	-10.4	-6.2	-3.5	0.20	3.2	0.9956
OW-200	-142.6	-51.6	-8.6	-5.0	-2.9	0.20	2.0	0.9935
OW-250	-142.5	-52.7	-9.7	-6.3	-4.0	0.20	2.5	0.9910
OW-300	-178.4	-65.0	-11.2	-6.9	-4.2	0.18	2.1	0.9983
2,4-DNP								
Unpyrolyzed	-48.1	-19.2	-3.5	-2.3	-1.9	0.30	4.7	0.9991
OW-100	-82.2	-30.0	-4.9	-3.9	-1.5	0.24	1.5	0.9631
OW-150	-94.1	-33.8	-5.2	-3.6	-1.4	0.26	3.4	0.9984



Table 3 continued

	ΔS° (J K ⁻¹ mol ⁻¹)	ΔH° (kJ mol ⁻¹)	ΔG° (kJ mol ⁻¹)			k_{id} (g mg ⁻¹ min ^{-0.5})	Second order	
			30 °C	50 °C	70 °C		k_2 (×10 ⁻³) (g mg ⁻¹ min ⁻¹)	R^2
OW-200	-98.0	-34.6	-4.8	-3.2	-0.9	0.30	2.6	0.7675
OW-250	-71.4	-26.4	-4.7	-3.7	-1.8	0.20	4.0	0.9994
OW-300	-71.3	-26.5	-4.9	-3.6	-2.0	0.26	4.7	0.9997

**Fig. 4** Intraparticle diffusion plots for the adsorption of **a** 2-CP and **b** 4-CP on pyrolyzed olive wood adsorbents

The values of k_{id} of the pyrolyzed olive wood were very close to those values reported by Aravindhan et al. (2009) for the adsorption of phenol on green macro-alga, and those reported by Wu and Yu (2006) for the adsorption of 2,4-dichlorophenol on *Phanerochaete chrysosporium*.

The kinetic parameters for the adsorption of phenols pyrolyzed-then-ethanol-washed sorbents are shown in Table 4. It was noted that, compared to the pyrolyzed only olive wood sorbents, k_2 decreased for Ph and 2-NP but increased for 2-CP, 3-CP, 4-CP, 4-NP and 2,4-DNP.

According to the Morris–Weber equation, the pyrolyzed-then-ethanol-washed sorbents gave higher k_{id} values for all phenols (except Ph), which indicated that the intraparticle diffusion step became faster and thus has a less effect as a rate-limiting step.

Thermodynamic considerations

According to the thermodynamic parameters presented in Table 3, adsorption of phenols on unpyrolyzed olive wood was generally exothermic as indicated by negative ΔH° values. The adsorption process was spontaneous at 30 °C, but the spontaneity of the adsorption decreases at higher temperatures as indicated by ΔG° values that became less negative. The randomness decreased after adsorption as indicated by the negative values of ΔS° .

The effect of pyrolysis of olive wood on its adsorption thermodynamic parameters toward various phenols is shown in Table 3. The results were compared with the unpyrolyzed olive wood sorbent. It was noted that $\ln K_c$ (which represent the favorability, capacity and ability of the adsorbent to retain adsorbate) increased for all the phenols at all the temperatures. Consequently, the spontaneity of the reaction (expressed by the increase in negativity of ΔG° values) has increased for all the phenols. The values of ΔG° lie within the physical adsorption range (from -20 to 0 kJ mol⁻¹). The adsorption process became more exothermic for all the phenols after pyrolysis except for Ph. This was indicated by the negative increase in ΔH° values. The randomness of the adsorption process increased for Ph and 2-NP. This was reflected by the increase in ΔS° values. On the contrary, the randomness of the adsorption process decreased for 2-CP, 3-CP, 4-CP, 4-NP and 2,4-DNP.

Thermodynamic parameters for the pyrolyzed-ethanol-washed olive wood are presented in Table 4. Compared to the pyrolyzed only olive wood sorbents, it was noted that adsorption became less spontaneous as indicated by less negative ΔG° values. Furthermore, less negative ΔH° values indicated less exothermic adsorption for the phenolic compounds after washing the pyrolyzed olive wood sorbents (except for Ph). By following ΔS° values, it was noted that the randomness of the adsorption process increased for all the phenols except for Ph.

Table 4 Parameters of adsorption kinetics and thermodynamics of pyrolyzed-ethanol-washed olive wood sorbents

	ΔS° (J K ⁻¹ mol ⁻¹)	ΔH° (kJ mol ⁻¹)	ΔG° (kJ mol ⁻¹)			k_{id} (g mg ⁻¹ min ^{-0.5})	Second order	
			30 °C	50 °C	70 °C		k_2 ($\times 10^{-3}$) (g mg ⁻¹ min ⁻¹)	R^2
Ph								
OW-100-ethanol	-107.5	-37.4	-4.7	-2.9	-0.3	0.26	2.2	0.9990
OW-150-ethanol	-103.3	-35.8	-4.3	-2.8	-0.1	0.16	1.9	0.9990
OW-200-ethanol	-106.5	-36.1	-3.9	-1.5	0.3	0.28	2.8	0.9991
OW-250-ethanol	-89.9	-30.8	-3.7	-1.4	-0.2	0.14	1.5	0.9964
OW-300-ethanol	-115.0	-39.4	-4.7	-1.8	-0.1	0.20	2.1	0.9970
2-CP								
OW-100-ethanol	23.1	2.5	-3.8	-6.6	-4.5	0.46	7.7	0.9998
OW-150-ethanol	22.0	2.5	-3.5	-6.3	-4.1	0.56	6.3	0.9997
OW-200-ethanol	2.7	-3.0	-3.0	-5.7	-2.9	0.56	4.2	0.9998
OW-250-ethanol	16.9	1.1	-3.3	-5.9	-3.8	0.42	9.1	0.9998
OW-300-ethanol	11.6	-0.9	-3.8	-6.1	-4.1	0.38	10.9	0.9998
3-CP								
OW-100-ethanol	-119.0	-42.2	-6.3	-3.3	-1.6	0.16	6.7	0.9994
OW-150-ethanol	-104.2	-36.9	-5.6	-2.6	-1.5	0.20	8.7	0.9958
OW-200-ethanol	-115.1	-40.1	-5.4	-2.3	-0.9	0.18	4.1	0.9956
OW-250-ethanol	-88.4	-31.7	-5.3	-2.4	-1.8	0.16	4.4	0.9991
OW-300-ethanol	-92.0	-33.2	-5.6	-2.7	-2.1	0.26	6.7	0.9921
4-CP								
OW-100-ethanol	-115.3	-40.2	-5.4	-2.6	-0.8	0.48	8.8	0.9999
OW-150-ethanol	-114.3	-39.8	-5.3	-2.5	-0.7	0.44	23.2	1.0000
OW-200-ethanol	-114.4	-39.4	-4.8	-2.1	-0.3	0.40	2.4	0.9895
OW-250-ethanol	-104.5	-36.6	-5.1	-2.4	-1.0	0.38	10.2	0.9999
OW-300-ethanol	-123.7	-43.2	-5.9	-2.9	-1.1	0.38	8.0	0.9998
2-NP								
OW-100-ethanol	-73.1	-26.6	-4.3	-3.4	-1.3	0.22	3.9	0.9987
OW-150-ethanol	-75.5	-27.2	-4.2	-3.2	-1.1	0.28	3.8	0.9989
OW-200-ethanol	-69.9	-24.3	-3.1	-1.9	-0.2	0.34	4.1	0.9994
OW-250-ethanol	-80.5	-28.3	-3.8	-2.5	-0.6	0.26	2.6	0.9927
OW-300-ethanol	-79.6	-28.2	-3.9	-2.9	-0.7	0.38	5.3	0.9991
4-NP								
OW-100-ethanol	-119.8	-41.5	-5.4	-2.4	-0.6	0.48	9.9	0.9999
OW-150-ethanol	-110.8	-37.8	-4.4	-1.7	-0.1	0.50	24.5	1.0000
OW-200-ethanol	-111.8	-37.8	-4.0	-1.5	0.4.0	0.46	8.0	0.9999
OW-250-ethanol	-115.5	-39.9	-4.9	-2.4	-0.3	0.44	7.9	0.9999
OW-300-ethanol	-111.0	-38.2	-4.7	-2.2	-0.3	0.38	8.0	0.9998
2,4-DNP								
OW-100-ethanol	-54.8	-20.8	-4.2	-2.8	-2.1	0.32	10.3	0.9999
OW-150-ethanol	-69.8	-25.3	-4.2	-2.7	-1.5	0.16	3.2	0.9987
OW-200-ethanol	-66.6	-23.5	-3.5	-1.5	-0.8	0.22	3.8	0.9963
OW-250-ethanol	-69.4	-24.7	-3.8	-1.9	-1.0	0.24	5.3	0.9993
OW-300-ethanol	-61.1	-22.1	-3.7	-2.0	-1.3	0.24	4.6	0.9993

Conclusion

Pyrolysis of olive wood has positively affected adsorption capacity, favorability and spontaneity of phenolic compounds

on the pyrolyzed olive wood. The temperature of pyrolysis did not show any clear trend on the adsorption properties. Washing the pyrolyzed sorbents with ethanol has negatively affected the adsorption capacity, favorability and spontaneity. This

indicated that pyrolysis produced species on the surface that were responsible for the improved adsorption properties of the pyrolyzed olive wood. While this paper is important in its own right, the authors wish to make suggestions for further work. In particular, the authors feel that the process needs investigating in a scaled up form. Future experiments might include an investigation of the effects of different pyrolysis techniques; for example, partial pyrolysis before the grinding might be equally effective and, in practice, might make the required grinding process less demanding of energy. It is also worthy to investigate how the partial pyrolysis might be achieved to provide sorbents for use in real water treatment situations.

Acknowledgments The authors are grateful for the Faculty of Graduate Studies and Scientific Research at the Hashemite University for supporting this project.

References

- Abia AA, Horsfall M, Didi O (2003) The use of chemically modified and unmodified cassava waste for the removal of Cd, Cu and Zn ions from aqueous solution. *Bioresour Technol* 90:345–348
- Ahmaruzzaman M (2008) Adsorption of phenolic compounds on low-cost adsorbents: a review. *Adv Colloid Interface* 143:48–67
- Aravindhan R, Rao JR, Nair BU (2009) Application of a chemically modified green macro alga as a biosorbent for phenol removal. *J Environ Manag* 90:1877–1883
- Bansode RR, Losso JN, Marshall WE, Rao RM, Portier RJ (2004) Pecan shell-based granular activated carbon for treatment of chemical oxygen demand (COD) in municipal wastewater. *Bioresour Technol* 94:129–135
- Bayramoglu G, Gursel I, Tunali Y, Arica MY (2009) Biosorption of phenol and 2-chlorophenol by *Funalia trogii* pellets. *Bioresour Technol* 100:2685–2691
- Brandt S, Zen AP, Deckwer WD (1997) Adsorption and desorption of pentachlorophenol on cells of *Mycobacterium chlorophenolicum* PCP-1. *Biotechnol Bioeng* 55:480–489
- Bridgwater AV (1994) Thermogravimetric analysis of the components of biomass: advances in thermochemical biomass conversion. Blackie Academic and Professional, London
- Cruz CCV, Da Costa ACA, Henriques CA, Luna AS (2004) Kinetic modeling and equilibrium studies during cadmium biosorption by dead *Sargassum* sp. *Biomass. Bioresour Technol* 91:249–257
- de Hoces MC, de Castro FH, Garcia GB, Rivas G (2006) Equilibrium modeling of removal of cadmium ions by olive stones. *Environ Prog* 25:261–266
- El-Sheikh AH, Newman AP, Al-Daffae H, Phull S, Cresswell N (2004) Characterization of activated carbon prepared from a single cultivar of *Jordanian* olive stone by chemical and physicochemical techniques. *J Anal Appl Pyrol* 71:151–164
- El-Sheikh AH, Alzawahreh AM, Sweileh JA (2011) Preparation of an efficient sorbent by washing then pyrolysis of olive wood for simultaneous solid phase extraction of chloro-phenols and nitro-phenols from water. *Talanta* 85:1034–1042
- Fourest E, Volesky B (1997) Alginate properties and heavy metal biosorption by marine algae. *Appl Biochem Biotechnol* 67:215–226
- Freundlich HMF (1906) Liber die adsorption in lösungen. *Phys Chem* 57:385–470
- Frimmel FH, Huber L (1996) Influence of humic substances on the aquatic sorption of heavy metals on defined minerals phases. *Environ Int* 22:507–517
- Giles CH, Smith DA (1974) General treatment and classification of the solute sorption isotherms. *J Colloid Interface* 47:755–765
- Grioui N, Halouani K, Zoulalian A, Halouani F (2007) Experimental study of thermal effect on olive wood porous structure during carbonization. *Maderas Ciencia y tecnología* 9:15–28
- Hajaligol M, Waymack B, Kellogg D (2002) Pyrolysis behaviour and kinetics of biomass derived materials. *J Anal Appl Pyrol* 62:331–349
- Ho YS, McKay G (2000) The kinetics of sorption of divalent metal ions onto sphagnum moss peat. *Water Res* 34:735–742
- Igwe JC, Nwokennaya EC, Abia AA (2005) The role of pH in heavy metal detoxification by biosorption from aqueous solutions containing chelating agents. *Afr J Biotechnol* 4:1109–1112
- Khan AR, Singh RP (1987) Adsorption thermodynamics of carbofuran on Sn(IV) arsenosilicate in H⁺, Na⁺ and Ca²⁺ forms. *Colloid Surface A* 24:33–42
- Lagergren S (1898) Zur theorie der sogenannten adsorption gelöster stoffe. *K Sven Vetenskapskad Handl* 24:1–39
- Langmuir I (1918) The adsorption of gases on plane surfaces of glass, mica, and platinum. *JACS* 40:1361–1368
- Martin-Lara MA, Pagnanelli F, Mainelli S, Calero M, Toro L (2008) Chemical treatment of olive pomace: effect on acid-base properties and metal biosorption capacity. *J Hazard Mater* 156:448–457
- Mathialagan T, Viraraghavan T (2008) Biosorption of chlorophenols: a review. *Int J Environ Pollut* 34:164–194
- Nadavala SK, Swayampakula K, Boddu VM, Abburi K (2009) Biosorption of phenol and *o*-chlorophenol from aqueous solutions on to chitosan–calcium alginate blended beads. *J Hazard Mater* 162:482–489
- Navarro AE, Portales RF, Sun-Kou MR, Llanos BP (2008) Effect of pH on phenol biosorption by marine seaweeds. *J Hazard Mater* 156:405–411
- Overend RP, Chornet E (1999) 4th conference on biomass: a growth opportunity in green energy and value-added products. Pergamon-Elsevier Science, Oxford
- Pan B, Xing B (2008) Adsorption mechanisms of chemicals on carbon nanotubes. *Environ Sci Technol* 42:9005–9013
- Perez-Bonilla M, Salido S, van Beek TA, Linares-Palomino PJ, Altarejos J, Nogueras M, Sanchez A (2006) Isolation and identification of radical scavengers in olive tree (*Olea europaea*) wood. *J Chromatogr A* 1112:311–318
- Raji C, Amirudhan TS (1998) Batch Cr(VI) removal by polyacrylamide-grafted saw dust: kinetics and thermodynamics. *Water Res* 32:3772–3780
- Saka C, Sahin O, Küçük MM (2012) Applications on agricultural and forest waste adsorbents for the removal of lead (II) from contaminated waters. *Int J Environ Sci Technol* 9:379–394
- Sanchez AG, Ayuso EA, De Blas OJ (1999) Sorption of heavy metals from industrial waste water by low-cost mineral silicates. *Clay Miner* 34:469–477
- Shin EW, Karthikeyan KG, Tshabalala MA (2005) Orthophosphate sorption onto lanthanum-treated lignocellulosic sorbents. *Environ Sci Technol* 39:6273–6279
- US Environmental Protection Agency (1988) Technology screening guide for treatment of CERCLA soils and sludges. Publication EPA/540/2-88/004, Washington DC
- Vazquez G, Gonzalez-Alvarez J, Garcia AI, Freire MS, Antorrena G (2007) Adsorption of phenol on formaldehyde-pretreated *Pinus pinaster* bark: equilibrium and kinetics. *Bioresour Technol* 98:1535–1540
- Weber WJ, Morris JC (1963) Kinetics of adsorption on carbon from solution. *J Sanit Eng Div* 89:31–39
- Wu J, Yu H (2006) Biosorption of 2,4-dichlorophenol from aqueous solution by *Phanerochaete chrysosporium* biomass: isotherms, kinetics and thermodynamics. *J Hazard Mater* 137:498–508
- Zghida H, Gauthier R, Helal A, Bartegi A (2006) Modeling of adsorption of anionic surfactants onto cationized lignocellulosic materials. *J Appl Polym Sci* 99:82–87